Mathematical modelling of mass transfer of paramagnetic ions through an inert membrane by the transient magnetic concentration gradient force

John A. Svendsen,* and Magne Waskaas
University of South-Eastern Norway, Faculty of Technology, Natural Sciences and Maritime Sciences, Kjølnes Ring 56, 3901 Porsgrunn, Norway

Author information
Corresponding Author
Phone: +47 91854847, Fax: not used at USN
E-mail: john.arild.svendsen@hotmail.com or (john.a.svendsen@usn.no)

ABSTRACT
The objective of this work is to suggest a mathematical model for mass-transfer of a paramagnetic electrolyte, nickel(II)chloride solution, through an inert, thin membrane from one chamber to another under influence of magnetic fields which is applied perpendicular to the membrane. The model is based on the magnetic concentration gradient force, the Fick's law of diffusion, and the Hagen-Poiseuille law for paramagnetic ion transport in the membrane. The magnetic concentration gradient force is found to be elusive and points in the direction of the magnetic field, in our case, the direction of the Fick diffusion flux. The reason is the gradient of the magnetic volume susceptibility for the electrolyte in the membrane, which decreases in the direction of the magnetic field. This is in accordance to the variable-reluctance principle. Mass balances for transport of Ni ions in distilled water through the membrane is derived, and is governed by a partial differential equation in one-dimensional space and time with specified initial and boundary conditions. The associated flux is superimposed on the pure Fick diffusion flux. The total flux is described by a nonlinear partial differential equation, which has not previously been used to describe transfer phenomena in paramagnetic solutions in magnetic fields. The simulated results were compared with experimental results and coincide approximately in all points for unstirred solutions. In stirred solutions, where the mass transfer coefficient at the membrane inlet approaches infinity if ideal mixing, no experimental or simulated effect was observed of the magnetic field.

Keywords
magnetic force; electrolyte; nonlinear diffusion; mass balance; inert membrane

1. Introduction

The influence of static magnetic fields on electrochemical processes has been studied over decades. The reported experimental and theoretical results include effects on electrode kinetics, the morphology of deposits on electrodes, dissolution of metal electrodes and mass-transfer. Several reviews have been carried out.[1-9] Three magnetic driving forces which could be responsible for the observed effects, are purposed: the Lorentz force, the magnetic field gradient force, and the magnetic concentration gradient force. The Lorentz force which is due to the interaction of a magnetic field with an electric current, is accepted as the main driving force for the magnetic field effects in electrochemical systems. The magnetic field gradient force which is due to a field gradient in electrochemical systems when the field is non-uniform, has been investigated and discussed by several groups as well. Their results show a transport of paramagnetic species in electrolytical solutions toward regions of higher magnetic flux densities when exposed to inhomogeneous static magnetic fields.[10-16]

The magnetic concentration gradient force, also denoted the paramagnetic gradient force or the paramagnetic force, arises when a paramagnetic electrolyte, with a gradient in its magnetic susceptibility, is subjected to a magnetic field. A gradient in the magnetic susceptibility arises for example at an electrode/electrolyte interface where paramagnetic ions are produced or consumed. This electrode/electrolyte interface is denoted the diffusion layer.[17]

Mass-transfer due to the possible paramagnetic concentration gradient force for anodic or cathodic electrode reactions, have been studied by many groups. They used electrochemical cells consisted of vertical electrodes immersed in paramagnetic or diamagnetic electrolytes. The magnetic fields were applied perpendicular to the electrode surfaces. The dynamic electrode reactions were analyzed by well-known methods, including voltammetry which involves applied currents that are either parallel or perpendicular to the magnetic fields. These results show an enhanced mass transfer by enhanced convection in the vicinity of the electrode due to the magnetic fields. The results are explained in terms of the Lorentz force and in terms of the additional magnetic concentration gradient force which may interact with natural convection. The suggested direction of the force given by these authors is in the same direction as increasing magnetic susceptibility. The effect appears to depend on the field-direction relative to the electrode surface and the applied current, and the cell geometry and experimental setup.[13,18-33]

Natural, or free, convection is caused by density variations in the solution which arises from concentration variations at the surface of the electrode.[34] Ragsdale and White showed that the driving force for natural

convection is in the same order of magnitude as magnetic forces and may interact with each other.[35]

However, the role of the magnetic concentration gradient force for mass-transfer in electrochemical systems, has been questioned, mainly, because of its small magnitude relative to the driving force for diffusion.[6,36]

Results from experiments under open circuit conditions, i.e. without any applied currents, indicate that rest potentials of iron electrodes in ferric electrolytes shifted in noble direction when exposed to magnetic fields. The results are discussed with respect to the magnetic concentration gradient force arises from the gradient in the ferric concentration at the electrode surface and to the Lorentz force.[37-43]

Leventis and Gao[44], Leventis and Dass[45] and Leventis et al[46] demonstrated that paramagnetic ions produced by an electrode, form a diffusion layer with highest concentration at the solution/electrode interface and fade away in the bulk by natural convection. When a homogeneous magnetic field of 3.3 T was applied perpendicular to either a vertical or a horizontal electrode surface, the paramagnetic ions were held close to the electrode surface. The demonstrations were supplemented by voltammetry. The results were discussed and explained in terms of the magnetic concentration gradient force, which was directed toward the electrode, and opposed the natural convection.

Waskaas[47] studied possible short-term effect of a homogeneous magnetic field on mass-transfer of paramagnetic ions through a vertical inert membrane. The magnetic fields (up to 0.82 T) were oriented horizontally and parallel to the transport direction. The results showed an increased mass transfer through the membrane due to the magnetic field. A magnetic driving force responsible for this effect was suggested. The force was based on the gradient of the magnetic susceptibility in the solution in the membrane, i.e. the later called magnetic concentration gradient force. The suggested direction of the force was in the same direction as decreasing magnetic susceptibility. The argumentation was based on the variable-reluctance principle, i.e. the principle that an unrestrained piece of magnetic material will move to complete a magnetic flux path with minimum reluctance. Similar results were obtained by another group.[48]

The results of the literature survey show that the magnetic concentration gradient force does exist. The force arises when a paramagnetic electrolyte with a gradient in its magnetic susceptibility, is subjected to a magnetic field. The force appears to be elusive and may interact with natural convection and cause additional mass transfer. However, several questions remain unanswered at present, including the actual

phenomenon of the force and its interactions with mass transfer in electrolytic solutions.

The objective of this work is to suggest a mathematical model for mass transfer of a paramagnetic electrolyte through an inert, thin membrane under influence of magnetic fields in unstirred and stirred solutions. The suggested magnetic driving force is the magnetic concentration gradient force. In addition, the direction of the force, will be discussed. Simulated values of the mass transfer will be compared to experimental values.

2. Experimental

The experimental setup is shown in Fig. 1a. The system consisted of an electromagnet, a He-Ne Laser, a photometer and an exposure chamber. Photos of the exposure chamber is shown in Fig. 1b and Fig. 1c. The exposure chamber contained two chambers (1 and 2) separated by an inert membrane. Initially, chamber 1 was filled with Ni ions dissolved in distilled water, and chamber 2 was filled with only distilled water. The experimental setup and methods are explained in detail elsewhere by Waskaas.[47]

The exposure chamber was placed in the gap of the electromagnet, which was supplied by a constant current source. The diameter of the pole shoes was 10.0 cm. The gap between them was 3.0 cm. The magnetic circuit consisted of the electromagnet with constant magnetomotive force, NI, where N is number of windings and I is a constant current, and the expose chamber, including the chambers 1 and 2 and the inert membrane. The magnetic flux density in the gap was selected between 0 and 0.8 T. The field was mapped and was found to be homogeneous where the membrane was placed. The dimension of the system is shown in Appendix B, Table 3.

2.1. The system and the environment

The system consists of the paramagnetic electrolyte of Ni ions in distilled water in the two chambers, the channel in front of the inert membrane and the inert membrane.

The environment is the electromagnet which generate a constant magnetic field B directed normal to the membrane front side. The chambers are not heat insulated. Both the current in the electromagnet and joule heating accompanied by the motion of the Ni ions in a magnetic field generates heat and a noticeable temperature increase after about 730 seconds. This is the reason the experiments were stopped after 705 seconds. In each experiment the concentration of Ni ions in chamber 2 was measured (detected) every 1.5 seconds. Each experiment was repeated seven times, and the average concentration of Ni in chamber 2

at fixed times was calculated, together with variance and standard deviation. The experiments were carried out under both stirred and unstirred conditions. In Waskaas[47] it was shown that the effect of B was negligible under stirred conditions but this was not the case under unstirred conditions. All cases simulated show the approximately unstirred conditions. The experimental results are shown in Appendix F.

Fig. 1.

3. Theory

Assume mass transfer of a paramagnetic electrolyte through an inert membrane under influence of a magnetic B field directed perpendicular to the membrane, as shown in Fig. 1a.

3.1. Definition of the mathematical system

In the mathematical sense, the membrane filled with liquid and Ni ions in the membrane, together with its initial and boundary conditions, constitute the system as shown in Fig. 2. It is assumed that the magnetic field B is constant and directed perpendicular to the membrane. The positive x-direction is from left to right, in the direction of Fick diffusion. The two chambers and the membrane constitute the system in our case, and the electromagnet producing the magnetic field B is denoted the environment.

3.2. Assumptions

The diameter of the membrane pores is much larger than the diameter of the Ni ions and the diameter of the water molecules.
Water is in great abundance and moves through the membrane by equimolar counter-diffusion. Hence, the water velocity is much smaller than the velocity of the Ni ions and has been ignored in the final calculation. The hydrostatic pressure is constant.

It is further assumed that the migration/diffusion process is due to two mechanisms: Fick diffusion and migration due to the magnetic concentration gradient force in a constant and homogeneous magnetic field B. The concentration of the solution, c_s, and density, ρ_s, are everywhere assumed to be approximately constant because of the large difference between the concentration of water (55.5 M), compared to the concentration of the Ni ions (0.5, 1.0 and 2.0 M). The words distilled water and water are used interchangeably in this article.

Fig. 2.

Chamber 1, the inert membrane and chamber 2 constitute the exposure chamber. Assume that the exposure chamber is placed in the gap of the electromagnet, which apply a constant magnetomotive force, NI, i.e. constant current, I, through the electromagnet's windings. The exposure chamber is part of the magnetic circuit. Initially, chamber 1 was filled with Ni ions and distilled water to either 0.5, 1.0 or 2.0 M of $NiCl_2$. The membrane and chamber 2 were filled with distilled water only. Diffusion starts, and finally the concentrations reach steady state in chamber 1, the membrane and chamber 2.[17,47]

The concentration of $NiCl_2$ in both chamber 1 and chamber 2 is assumed to be ideally mixed and hence only depends on time, $c_1(t)$ and $c_2(t)$ respectively. In the membrane however, the concentration of $NiCl_2$ is distributed and denoted c(x,t). In equations regarding the membrane, c(x,t) is usually denoted c, for ease of readability.

The initial concentration of $NiCl_2$ in chamber 1 is uniform and denoted $c_1(0) = c_{10}$. The value is either 0.5, 1.0 or 2.0 mol/dm^{-3}. The initial concentration of $NiCl_2$ in chamber 2 is in all cases zero and denoted $c_2(0) = c_{20} = 0$ mol/dm^{-3}. In the membrane, the initial concentration of $NiCl_2$ is also zero in all cases and is denoted $c_m(x,0) = 0$ mol/dm^{-3}.

The initial concentrations in mol/liter in respectively chamber 1, the membrane and the chamber 2 were

$$c_1(0)= c_{10},\ c(0,0) = 0 \text{ and } = c_2(0)= 0 \qquad (1)$$

3.3. The energy density and the corresponding force

The energy density stored in a magnetic field *B* in a magnetic material with magnetic permeability, μ, is given in for example Reitz et al.:[49]

$$E_m = \frac{B^2}{2\mu} \qquad (2)$$

For the case where the material is a paramagnetic electrolyte with concentration c, and magnetic molar susceptibility χ_{mol}, the magnetic permeability μ is given by:[50,51]

$$\mu = \mu_0(1 + \chi_{mol}c) \qquad (3)$$

Here, μ_0 is the magnetic permeability for vacuum.

If the geometry of the magnetic circuit is changed by moving one part and the applied current to the electromagnet is constant, the force per unit

volume on the moving part is the gradient of the magnetic energy per unit volume:[49]

$$F_m = \nabla E_m \tag{4}$$

For movement in the x-direction with constant current I:

$$F_m = \left(\frac{\partial E_m}{\partial \mathrm{x}}\right)_I \tag{5}$$

The total energy per unit liquid volume E is defined and reads[52,53]

$$E = E_m + U + E_k + E_p \tag{6}$$

Here, U, E_k and E_p are respectively the internal energy, the kinetic energy and the potential energy, all per unit liquid volume. The change in dE/dx is derived in Appendix C. It shows that $dE/dx \approx dE_m/dx$. Consequently, $dE \approx dE_m$.

The first law of thermodynamics reads:[54]

$$\mathrm{dE} = \mathrm{d'Q} - \mathrm{d'W} \tag{7}$$

The symbol d' is used in Eq. (7) to indicate that Q and W are inexact differentials since heat Q and work W are both path-dependent.
In our case, the environment (the magnetic field B) exerts work on the system (i.e. the electrolyte in the chambers) by forcing the paramagnetic Ni ions through the inert membrane. According to the standard definition in physics, work W is positive if the system exerts work on the environment and negative if the environment exerts work on the system. In the time period of each experiment the system was approximately adiabatic, so d'Q ≈ 0. Hence, Eq. (7) becomes

$$\mathrm{dE}_m = -\mathrm{d}'(-\mathrm{W}) = d'W = F_m dx \tag{8}$$

From Eq. (8) it follows that the magnetic concentration gradient force per unit volume is

$$F_m = \frac{\mathrm{dE}_m}{\mathrm{dx}} \tag{9}$$

3.4. The paramagnetic force acting on the Ni ions

In our case the electrolyte within the membrane is the moving part of the magnetic circuit. Since the magnetomotive force is constant, i.e. the current I through the electromagnet is constant. The Ni concentration c in the membrane is a function of x and time t. There is a concentration gradient of Ni in the inert membrane and hence, a gradient in the

magnetic volume susceptibility (κ) in the electrolyte in the membrane. Notice however, that the magnetic molar susceptibility (χ_{mol}) is used in this model, see Appendix D. The magnetic concentration gradient force per unit volume acting on the electrolyte when the magnetic field B is constant, is obtained by combining Eqs. (2), (3) and (9). Using the chain rule and that
$1+\kappa = 1+\chi_{\mathrm{mol}}c \approx 1$, the result becomes

$$F_m = \frac{\partial \mathrm{E}_m}{\partial \mathrm{x}} = \frac{\partial}{\partial \mathrm{x}}\left[\frac{B^2}{2\mu_0(1+\chi_{\mathrm{mol}}c)}\right] = -\frac{\chi_{\mathrm{mol}}\mathrm{B}^2}{2\mu_0\,(1+\chi_{\mathrm{mol}}c)^2}\frac{\partial \mathrm{c}}{\partial \mathrm{x}} \approx -\frac{\chi_{\mathrm{mol}}\mathrm{B}^2}{2\mu_0}\frac{\partial \mathrm{c}}{\partial \mathrm{x}} \tag{10}$$

If in addition the magnetic field depends on position x, Eq. (9) and Eq. (10) must include the magnetic field gradient force per unit volume. In that case F_m becomes

$$F_m = -\frac{\chi_{\mathrm{mol}}cB}{\mu_0}\frac{\partial \mathrm{B}}{\partial \mathrm{x}} - \frac{\chi_{\mathrm{mol}}\mathrm{B}^2}{2\mu_0}\frac{\partial \mathrm{c}}{\partial \mathrm{x}} \tag{11}$$

In our case $\frac{\partial \mathrm{B}}{\partial \mathrm{x}} = 0$. Hence, only the second term on the right hand side of Eq. (11) is used in this article.

This is in accordance with reluctance considerations of the electrolyte within the membrane. According to Gauss' law of Maxwell's equations, electromagnets, or permanent magnets, set up magnetic flux lines that form closed loops and define a magnetic circuit.[49] The magnetic flux is determined by the magnetomotive force and the reluctance of the magnetic circuit. The average reluctance in the membrane, $\overline{\mathcal{R}}$, is given by:[55]

$$\overline{\mathcal{R}}(x) = \frac{L_m}{\overline{\mu}A_{lm}} = \frac{L_m}{\mu_0\left[1+\chi_{\mathrm{mol}}\frac{(c_1+c)}{2}\right]A_{lm}} \tag{12}$$

In Eq. (12) it is assumed that c_1 is constant or approximately constant. This is verified in the second column in Table 2.

If the magnetic field B points in the positive x-direction as in Fig. 3a, then

$$\frac{\partial \overline{\mathcal{R}}}{\partial \mathrm{x}} = \frac{\partial}{\partial \mathrm{x}}\left[\frac{L_m}{\mu_0\left[1+\chi_{\mathrm{mol}}\frac{(c_1+c)}{2}\right]A_{lm}}\right] = -\frac{\frac{\chi_{mol}L_m}{2}}{\mu_0 A_{lm}\left[1+\chi_{\mathrm{mol}}\frac{(c_1+c)}{2}\right]^2}\frac{\partial \mathrm{c}}{\partial \mathrm{x}} > 0, \text{ since } \frac{\partial \mathrm{c}}{\partial \mathrm{x}} < 0 \tag{13a}$$

The square term in the denominator of Eq. (13a) is approximately 1, so the following approximation is valid

$$\frac{\partial \overline{\mathcal{R}}}{\partial \mathrm{x}} \approx -\frac{\chi_{mol}L_m}{2\mu_0 A_{lm}}\frac{\partial \mathrm{c}}{\partial \mathrm{x}} > 0, \text{ since } \frac{\partial \mathrm{c}}{\partial \mathrm{x}} < 0 \tag{13b}$$

If the magnetic field B points in the negative x-direction, Fig. 3b, then B points in the y-direction, where y = L_m- x, and dy = -dx in Eq. (13c).

$$\frac{\partial \overline{\mathcal{R}}}{\partial \mathrm{y}} = \frac{\partial}{\partial(-\mathrm{x})}\left[\frac{L_m}{\left[1+\chi_{\mathrm{mol}}\frac{(c_1+c)}{2}\right]A_{lm}}\right] \approx \frac{\chi_{\mathrm{mol}} L_m}{2\mu_0 A_{lm}}\frac{\partial \mathrm{c}}{\partial \mathrm{x}} \quad < 0 \quad , \quad \text{since } \frac{\partial \mathrm{c}}{\partial \mathrm{x}} < 0 \tag{13c}$$

It readily follows that in our case

$$\frac{\partial \overline{\mathcal{R}}}{\partial \mathrm{t}} \approx -\frac{\chi_{mol} L_m}{2\mu_0 A_{lm}}\frac{\partial \mathrm{c}}{\partial \mathrm{t}} \quad < 0, \quad \text{since } \frac{\partial \mathrm{c}}{\partial \mathrm{t}} > 0 \tag{13d}$$

From Eq. (13d) if follows that the higher concentration of paramagnetic species in the membrane, the less reluctance, see case A in Fig. 3a.

According to the variable-reluctance principle, which, due to conservation of energy in a magnetic circuit, i.e. a constant magnetomotive force acts upon a moving part in such direction as to tend to decrease the reluctance of the magnetic circuit.[56,57] Consequently, the magnetic force on the electrolyte within the membrane is directed along the positive x-axis, Fig. 2 and Fig. 3a.

These arguments for suggested direction of the magnetic concentration gradient force do not appear to be in accordance with arguments given in other studies.[6,27,36,41]

Fig. 3.

Discussion of Case A in Fig. 3a:

The paramagnetic force per unit volume is given by Eq. (14), and the magnetic field B points in the positive x-direction. Hence,

$$F_m = -\frac{\chi_{\mathrm{mol}} \mathrm{B}^2}{2\mu_0}\frac{\partial \mathrm{c}}{\partial \mathrm{x}} = -k_m \frac{\partial \mathrm{c}}{\partial x} > 0 \text{ , since } \frac{\partial \mathrm{c}}{\partial \mathrm{x}} < 0 \tag{14}$$

It follows from Eq. (14) that

$$k_m = \frac{\chi_{\mathrm{mol}} \mathrm{B}^2}{2\mu_0} \tag{15}$$

Below dc/dx is substituted with $\partial c/\partial x$ since c varies with x and time t. Both at the start of the experiments and at steady-state, $\partial c/\partial x \approx 0$, and hence $F_m \approx 0$ at start and steady-state. The electrolyte temperature started to rise after about 705 s. The experiments were therefore stopped after 705 s to keep the experiments at adiabatic conditions. This is the reason why only the simulations were run to steady-state.

Discussion of Case B in Fig. 3b:

The paramagnetic force per unit liquid volume is given by Eq. (14), but the magnetic field B now points in the negative x-direction. Hence, dx is replaced by -dx and

$$F_m = -\frac{\chi_{mol} B^2}{2\mu_0}\frac{\partial c}{\partial(-x)} = \frac{\chi_{mol} B^2}{2\mu_0}\frac{\partial c}{\partial x} = k_m \frac{\partial c}{\partial x} < 0 \text{ , since } \frac{\partial c}{\partial x} < 0 \qquad (16)$$

Many authors write a positive constant in front of the concentration gradient ∇C, and write the paramagnetic force per unit volume as[10,11,28,29,32,36,58]

$$F_m = \frac{\chi_{mol} B^2}{2\mu_0}\nabla C \qquad (17)$$

but forget or omit to define the direction of ∇c. Equation (17) is only correct if $\nabla c > 0$ in the direction of the magnetic field B. If $\nabla c < 0$ in the direction of the magnetic field B, as in case A in Fig. 3a, the correct formula is given by Eq. (14).

From the discussion of Figs. 3a and 3b, the conclusion is that the magnetic concentration gradient force per unit volume, F_m, points in the direction of the magnetic field B. In our case the direction of the Fick diffusion flux j defines the positive x-direction of the flow, see Fig. 3a, Case A.

3.5. A constant magnetic field is applied to the electrolyte

The flow system discussed in this chapter is classified as a closed-open vessel.[52] It means that close to the membrane inlet, x=0-, there is a convective flow. It is given by v_m in Eq. (18). In addition it is allowed for a possible natural mass transfer coefficient k_1 for all cases, B ≥ 0. In the inert membrane both diffusion and convection v_m occur. Both chamber 1 and chamber 2 are regarded as ideal mixing tanks in the model. This not true in the beginning of the process but appears to be a good approximation after some minutes as discussed in Results and discussion.

First, assume that the constant magnetic field B points in the positive x-direction as shown in Fig. 2 and Fig. 3a, that is, from left to right. Mass diffusion always flows from high to low concentration. The magnetic concentration gradient force, F_m, exerted on the paramagnetic Ni ions in position x in the system is given by Eq. (14).

The diameter of a Ni ion is typical 1/500 of the pore diameter. The paramagnetic force per liquid volume unit, F_m, therefore gives rise to a Hagen-Poiseuille flow in the pores of the membrane, as shown in Appendix C. The average ion velocity through the inert membrane, v_m, is given by

$$v_m = \frac{R^2}{8\rho\eta} F_m = -\frac{R^2 B^2 \chi_{mol}}{16\rho\eta\mu_0}\frac{\partial c}{\partial x} = -k_v \frac{\partial c}{\partial x} > 0 \text{ when } \frac{\partial c}{\partial x} < 0 \tag{18}$$

It follows from Eq. (18) that parameter k_v is

$$k_v = \frac{R^2 B^2 \chi_{mol}}{16\rho\eta\mu_0} \tag{19}$$

R is the pore radius in the membrane, and η is the absolute viscosity of the electrolyte. The mole flux through the membrane, caused by v_m, is also time dependent and reads

$$j_v = v_m c = -k_v c \frac{\partial c}{\partial x} > 0 \tag{20}$$

If the magnetic field B points in the negative x-direction, F_m is given by Eq. (16), and the negative F_m and v_m reads

$$v_m = \frac{R^2}{8\rho\eta} F_m = \frac{R^2 B^2 \chi_{mol}}{16\rho\eta\mu_0}\frac{\partial c}{\partial x} = k_v \frac{\partial c}{\partial x} < 0 \text{ when } \frac{\partial c}{\partial x} < 0 \tag{21}$$

$$j_v = v_m c = k_v c \frac{\partial c}{\partial x} < 0 \text{ when } \frac{\partial c}{\partial x} < 0 \tag{22}$$

The total molar ion flux, j, through the membrane is

$$j = j_D + j_v \tag{23}$$

Including j_v, Fick's second law becomes

$$\frac{\partial c}{\partial t} = -\frac{\partial j}{\partial x} = -\frac{\partial j_D}{\partial x} - \frac{\partial j_v}{\partial x} = D\frac{\partial^2 c}{\partial x^2} \pm k_v\left[c\frac{\partial^2 c}{\partial x^2} + \left(\frac{\partial c}{\partial x}\right)^2\right] \tag{24}$$

Here, the minus sign in front of k_v is used if B points in the negative x-direction.

The nonlinear PDE, given by Eq. (24), can alternatively be written

$$\frac{\partial c}{\partial t} = D\left[1 \pm \frac{k_v c}{D}\right]\frac{\partial^2 c}{\partial x^2} \pm k_v\left(\frac{\partial c}{\partial x}\right)^2 \tag{25a}$$

A study of Eq. (25a) shows that the quadratic term can be ignored, at least in the cases presented here. This is shown in Fig. 6. In Appendix E it is derived that the quadratic term can be ignored. The simplified diffusion equation reads

$$\frac{\partial c}{\partial t} \approx D\left[1 \pm \frac{k_v c}{D}\right]\frac{\partial^2 c}{dx^2} = D_{eff}\frac{\partial^2 c}{dx^2} \quad , D_{eff} = D\left[1 \pm \frac{k_v c}{D}\right] \tag{25b}$$

Since c depends on both x and t, so does D_{eff}. In addition, the parameter k_v depends on several parameters, including B^2. In all our cases the positive sign is used.

In this article, Eq. (25a) and Eq. (25b) are solved only for the case where the magnetic field B points in the positive x-direction, which is in the direction of decreasing Ni concentration, as shown in Fig 3a. In that case, the initial and boundary conditions are chosen as follows.

Initial conditions

The initial concentration of Ni ions in the membrane reads

$$c(\mathrm{x}, 0) = 0 \qquad 0 \le x \le L_m \tag{26}$$

The initial concentration of Ni ions in chamber 1 is

$$c_1(0) = c_{10} \tag{27}$$

The initial concentration of Ni ions in chamber 2 is

$$c_2(0) = 0 \tag{28}$$

Hence, all Ni ions are stored in chamber 1 initially.

Boundary conditions

At the inlet of the membrane, x = 0, the mole balance is given by the mixed boundary condition, or sometimes denoted Danckwerts boundary condition.[52] The time dependent boundary condition reads

$$c_1(t)|_{x=0} = -\frac{D}{(k_1+v_m)}\frac{\partial c}{\partial x}|_{x=0} + c(0,t) \tag{29}$$

The mole flow of Ni ions out of the membrane at $x = L_{m-}$ is equal to the mole flow of Ni ions into chamber 2 at $x = L_{m+}$. This implies that the mass transfer coefficient $k_2 \to \infty$ at $x = L_{m+}$. The time dependent boundary condition at $x = L_m$ reads

$$c_2(t)|_{x=L_{m+}} = c(L_{m-}, t) \tag{30}$$

At steady-state, Eq. (30) becomes

$$\frac{\partial c}{\partial x}|_{x=L_m} = 0 \tag{31}$$

Equation (25a) or Eq. (25b), with its initial and boundary conditions, are solved numerically using subroutine DMOLCH.[59]

A t = 0 and x = 0, there is a discontinuity in the $NiCl_2$ concentration. The transition from $c(0,t)|_{x=0} = c_1(t)|_{x=0}$ to $c(0_+,0) = 0$ is not instantaneous, but is calculated smoothly using subroutine DC2HER and function DCSDER of the IMSL library.[59] The time in seconds needed for the smooth transition, td, is specified by the user, but it can be estimated in advance.

How this discontinuity is handled numerically in IMSL is explained below.

Due to the restrictions in the type of boundary conditions successfully processed by subroutine DMOLCH of IMSL library, it is necessary to provide the derivative boundary value function $\gamma'(t)$ at x = 0. The function $\gamma(t)$ at x = 0 makes a smooth transition for c(0,t), from the value $\gamma(0)$ = c_{10} at t = 0 to the value c(0,td) = 0 at t = td. The transition phase for $\gamma'(t)$ is computed by evaluating a cubic interpolating polynomial. For this purpose, the function DCSDER is used. The interpolation is performed as a first step in the user-supplied subroutine FCNBC which calculates the boundary conditions at x = 0 and x = L_m. At the boundary x = 0, the function and derivative values $\gamma(0)$ = c_{10}, $\gamma'(0)$ = 0, γ(td) = 0 and γ'(td) = 0 are used as input to the subroutine DC2HER to obtain the coefficients evaluated by DCSDER. At t > td, $\gamma'(t) = 0$.
At x = L_m the time dependent boundary condition c(L_m,t) is calculated by Eq. (30) using Eq. (39).

The molar flux at the inlet and outlet of the membrane is calculated from

$$j_1 = -D\,\frac{\partial c}{\partial x}|_{x=0} \tag{32}$$

$$j_2 = -D\,\frac{\partial c}{\partial x}|_{x=L_m} \tag{33}$$

The liquid volume of chamber 1 and 2 is V_{l1} and V_{l2} respectively. The effective cross-sectional area A_{lm} for flow in the membrane is given by

$$A_{lm} = \varepsilon_m\, W_m H_{lm} \tag{34}$$

Here, ε_m is the porosity (void) of the membrane.

The total mole balance for Ni ions in the system is also calculated numerically. The time dependent number of moles of Ni in chamber 1 (the reservoir including the channel) and in chamber 2 are calculated from

$$\frac{dn_1(t)}{dt} \approx \frac{n_1(t+\Delta t)-n_1(t)}{\Delta t} = -j_1 A_{lm}\ ,\ \lim\ \Delta t \to 0 \tag{35}$$

$$\frac{dn_2(t)}{dt} \approx \frac{n_2(t+\Delta t)-n_2(t)}{\Delta t} = j_2 A_{lm}\ ,\ \lim\ \Delta t \to 0 \tag{36}$$

The ordinary differential equations given by Eq. (35) and Eq. (36) are here solved numerically, using a simple explicit Euler algorithm as indicated.

The concentration $c_1(t)$ in chamber 1 is calculated from Eq. (37). The concentration $c_2(t)$ in chamber 2 is calculated from Eq. (39) for all $t > 0$.

The concentration of Ni ions, in respectively chamber 1 and 2, is given by

$$c_1(t) = \frac{n_1(t)}{V_{l1}} \tag{37}$$

$$\frac{dc_1(t)}{dt} = \frac{1}{V_{l1}}\frac{dn_1(t)}{dt} = -\frac{j_1 A_{lm}}{V_{l1}} \tag{38}$$

$$c_2(t) = \frac{n_2(t)}{V_{l2}} \tag{39}$$

$$\frac{dc_2(t)}{dt} = \frac{1}{V_{l2}}\frac{dn_2(t)}{dt} = \frac{j_2 A_{lm}}{V_{l2}} \tag{40}$$

The number of moles of Ni in the membrane n(t) and the average concentration c(t) reads

$$n(t) = V_{l1}c_1(t) - V_{l2}c_2(t) \tag{41}$$

$$c(t) = \frac{n(t)}{V_{lm}} \tag{42}$$

The inverse of the overall mass transfer coefficient for pure Fick diffusion in the membrane, k_{ov}, and mass transfer coefficient k_1 at the inlet, is given by

$$\frac{1}{k_{ov}} = \frac{1}{k_1} + \frac{L_m}{D} \tag{43}$$

The membrane was divided into 1001 points and 1000 equally spaced intervals. The dynamic time step was determined by subroutine DMOLCH[59] with output to file every second as specified by the user. The model is programmed in Fortran 77.

3.6. The total mole balance for Ni in the system

The concentrations $c_1(t)$, and $c_2(t)$ are solved numerically when j_1 and j_2 are calculated at the boundaries of the membrane. The Ni ions are stored in either chamber 1, the membrane or in chamber 2. The total amount of Ni ions, K, is constant through the experiment and is given by

$$V_{l1}c_1(t) + V_{lm}c(t) + V_{l2}c_2(t) = V_{l1}c_1(0) + V_{lm}c(0) + V_{l2}c_2(0) = K$$

(44)

At steady-state, $c_1 = \mathrm{c} = c_2$. The steady-state concentration reads

$$c_1 = \mathrm{c} = c_2 = \frac{K}{V_{l1}+V_{lm}+V_{l2}} = \frac{V_{l1}c_1(0)+V_{lm}\mathrm{c}(0)+V_{l2}c_2(0)}{V_{l1}+V_{lm}+V_{l2}} \tag{45}$$

The number of moles of Ni in each chamber 1 and 2 as function of time is given by

$$n_1(t) = V_{l1}c_1(t) \tag{46}$$

$$n_2(t) = V_{l2}c_2(t) \tag{47}$$

At steady-state, the number of moles of Ni in each chamber and in the membrane becomes

$$n_1 = \frac{V_{l1}}{V_{l1}+V_{lm}+V_{l2}}K \tag{48}$$

$$n_2 = \frac{V_{l2}}{V_{l1}+V_{lm}+V_{l2}}K \tag{49}$$

$$n = \frac{V_{lm}}{V_{l1}+V_{lm}+V_{l2}}K \tag{50}$$

4. Results and discussion

The objective of this work has been to study theoretically the effect of unidirectional magnetic fields on the diffusion rate of a paramagnetic Ni ions moving through an inert membrane under approximately unstirred conditions. The net result forces the Ni ions through the membrane in the specified x-direction. The concentration gradient of Ni ions through the inert membrane is set up by the concentration difference of Ni ions between chamber 1 and chamber 2. When the magnetic field is turned off, $B = 0\,T$, the transport of Ni ions from chamber 1 to chamber 2 through the membrane is explained solely by ordinary Fick diffusion with a natural mass transfer coefficient k_1 as shown in Eq. (29) with v_m = 0. When $B > 0$, an additional force identified as the magnetic concentration gradient force F_m appears in the membrane. The resulting velocity v_m of the Ni ions is proportional to F_m as shown in Eq. (18) and Eq. (29).

A nonlinear regression program was programmed in Fortran 77 to tune D, k_1 and td as shown in Table 1. A few trial and error runs, using the diffusion program, were needed to estimate good start values of D, k_1 and td for the regression program for each of the seven cases. The diffusion program was converted to a subroutine which is called by the regression program. The IMSL subroutine DRNLIN[59] was called by the in-house program MHD-REGRESSION. A 90 % confidence interval was calculated

for the parameters in each case. Table 1 shows the span of the values of D, k_1 and td for various initial concentrations of Ni and various magnitudes of the magnetic field B. These are typical values for diffusion in liquid.

The simulated values of the Ni concentration in chamber 2 almost coincide with the experimental results in Fig. 4 and Fig. 5 and Appendix F, where a static homogeneous magnetic field B causes a significant increase in the diffusion and migration rate of paramagnetic Ni ions through an inert membrane in unstirred solutions, due to the dependence of the magnetic susceptibility on both the concentration of Ni ions and its gradient in the membrane. A velocity is set up in the membrane by the magnetic concentration gradient force per unit volume, and it is proportional to the concentration gradient of Ni in the membrane and the square of the magnetic field intensity B.

Table 1. Parameters for Fig. 4 and Fig. 5.

$c_1(0)$ (M)	B (T)	D (m^2/s)	k_1 (m/s)	td (s)
0.5	0	$2.1 \cdot 10^{-9}$	$1.8 \cdot 10^{-5}$	300
1.0	0	$9.4 \cdot 10^{-10}$	$1.6 \cdot 10^{-5}$	300
2.0	0	$1.0 \cdot 10^{-9}$	$1.6 \cdot 10^{-5}$	300
0.5	0.67	$4.6 \cdot 10^{-9}$	$2.0 \cdot 10^{-5}$	300
1.0	0.67	$1.6 \cdot 10^{-9}$	$1.7 \cdot 10^{-5}$	300
2.0	0.67	$1.5 \cdot 10^{-9}$	$2.2 \cdot 10^{-5}$	300
1.0	0.82	$1.9 \cdot 10^{-9}$	$2.2 \cdot 10^{-5}$	150

Table 2. The mole distribution of Ni in chamber 1, 2 and the membrane for case 1 M and B = 0 T at approximately steady state (Fick diffusion).

Time (s)	n_1 (mol)	n_2 (mol)	n_m (mol)
0.0	$2.909 \cdot 10^{-2}$	0.0	0.0
12000	$2.864 \cdot 10^{-2}$	$4.456 \cdot 10^{-4}$	$8.423 \cdot 10^{-6}$

The Ni detector was placed in the middle of chamber 2. Hence, there is a system time delay td in the beginning of an experiment where Ni is not detected in chamber 2 due to non-ideal mixing initially. In Fig. 4 the measured time delay is shown to be in the order of 150 seconds. The initial average velocity of Ni ions in chamber 2 is typically

$$v_2 = \frac{0.5L_2}{150} = \frac{0.5 \cdot 6 \cdot 10^{-3}}{150} = 2 \cdot 10^{-5} \quad \text{(m/s)} \qquad (51)$$

The velocity v_2 is here of the same order of magnitude as the overall mass transfer coefficient k_{ov}, as shown below

$$\frac{1}{k_{ov}} = \frac{1}{k_1} + \frac{L_m}{D} = \frac{1}{2.0 \cdot 10^{-5}} + \frac{150 \cdot 10^{-6}}{1.0 \cdot 10^{-9}} = 5 \cdot 10^4 \quad \text{(s/m)} \qquad (52)$$

$$k_{ov} = \frac{1}{5 \cdot 10^4} = 2 \cdot 10^{-5} \quad \text{(m/s)} \qquad (53)$$

The reason why the mathematical model suggests a delay time of 300 s instead of 150 s is due to the fact that the model assumes that chamber 2 is an ideal mixing chamber at all times. This is approximately true only after the concentration wave out of the membrane has reached the wall in chamber 2. To obtain the same velocity v_2 we calculate

$$v_2 = \frac{L_2}{300} = \frac{6 \cdot 10^{-3}}{300} = 2 \cdot 10^{-5} \text{ (m/s)} \qquad (54)$$

The magnetic susceptibility of diamagnetic water is negative and much smaller in absolute value than the magnetic susceptibility of the paramagnetic Ni ions by a factor 342 as shown in Eq. (C7) in Appendix C. Hence, the magnetic force F_m per unit volume for water could be neglected. In addition, since the solution is fairly dilute in all cases, the diffusion of the water molecules could be neglected. Hence, the water was regarded as a stagnant component. These assumptions led to the conclusion that only the PDE for the Ni concentration through the membrane, $c(\mathrm{x},\mathrm{t})$, needs to be solved with its initial and boundary conditions.

After simulation of the three reference cases with B = 0 T, the effect of the static, magnetic field B on the diffusion was simulated for B = 0.67 T, and B = 0.82 T in the 1 M case. In the case 0.5 M and 2 M only B = 0.67 T was applied, the same as in the measurements by Waskaas.[47] As expected, the diffusion increased considerably when the magnetic field B increased.

The measurements were stopped after 705 s, because the temperature of the solution started to rise as it was heated by the energy released from the electromagnet.[47] Before 705 s the temperature in the solution was 20 $\pm$ 1 °C.

The simulated values of the Ni concentration in chamber 2 correspond very well to the measured values in Fig. 4 and Fig. 5. The degree of mixing in chamber 2 increases with time after the Ni ions reach the wall in chamber 2, at a distance of 0.6 cm from the outlet of the membrane. The simplified numeric solution almost coincide with the numeric solution as shown in Fig. 6. In stirred solutions, where the mass transfer coefficient at the membrane inlet increases with increasing mixing and approaches infinity at ideal mixing, no experimental or simulated effect was observed of the magnetic field. This may indicate that the span for D and k_1 given in Table 1 for various magnitudes of the magnetic field B, appear to be less, respective greater, than assumed. This has to be studied more carefully in the future.

Fig. 4.

Fig. 5.

In Fig. 6 the numeric solution using Eq. (25a) is compared to the simplified numeric solution using Eq. (25b) for two cases, 0.5 M and 0.67 T and 1 M and 0.86 T. In both cases the simplified numeric solution is almost coinciding with the numeric solution. Hence, Eq. (25b) can in many cases be used with negligible loss of accuracy.

Fig. 6.

5. Conclusions

The mathematical model for mass transfer of a paramagnetic electrolyte through a membrane in a magnetic field is based on the magnetic concentration gradient force, the Fick's law of diffusion, and the Hagen-Poiseuille law.

It is shown that the magnetic concentration gradient force is elusive and points in the direction of the magnetic field, in our case, the direction of the Fick diffusion flux. The reason is the gradient of the magnetic volume susceptibility for the electrolyte in the membrane, which decreases in the direction of the magnetic field in all studied cases. This is in accordance to the variable-reluctance principle.

The magnetic concentration gradient force gives rise to a Hagen-Poiseuille flow through the membrane, which is superimposed on the pure Fick's diffusion flux. The total flux is described by a nonlinear partial differential equation, which has not previously been used to describe transfer phenomena in paramagnetic solutions in magnetic fields.

It is shown that the square term in the partial differential equation can be neglected.

The magnetic field effect is shown to be proportional to the concentration gradient of the paramagnetic ions in the membrane and the square of the magnetic field.

The simulated results were compared with experimental results and coincide approximately in all points for unstirred solutions. In stirred solutions, where the mass transfer coefficient at the membrane inlet approaches infinity if ideal mixing, no experimental or simulated effect was observed of the magnetic field. This may indicate that the given span of the diffusion constant and the mass transfer coefficient in magnetic

fields appear to be less, respective greater, than assumed. This has to be studied more carefully in the future.

References

1. T.Z. Fahidy, in *Modern aspects of electrochemistry no. 32*, edited by B.E. Conway, J.O.M. Bockris, and R.E.White (Kluwer Academic/Plenum Publishers, New York, 1999), pp. 333-354.

2. G. Hinds, J.M.D. Coey, and M.E.G. Lyons, Electrochem. Commun. 3, 215 (2001).

3. C. O'Reilly, G. Hinds, and J.M.D. Coey, J.Electrochem. Soc. 148, C674 (2001).

4. A. Alemany and J.P. Chopart, in *Magnetohydrodynamics – Historical evolution and trends,* edited by S. Molokov, R. Moreau, and H.K. Moffatt (Springer, Dordrecht, The Netherlands, 2007), pp. 391-407.

5. L.M.A. Monson and J.M.D. Coey, Electrochemistry Commun. 42, 38 (2014). http://dx.doi.org/10.1016/j.elecom.2014.02.006

6. A. Hudoba and S. Molokov, Physics of Fluids, 28, 114103 (2016) https://doi.org/10.1063/1.4965448

7. C. Chahtuor, H. Ben Hamed, H. Beji, A. Guizani and W. Alimi, Physics of Fluids, 30, 013101 (2018) https://doi.org/10.1063/1.5017996

8. S. Sarkar, S. Ganguly and M. Mishra, Physics of Fluids, 31, 082102 (2019) https://doi.org/10.1063/1.5112373

9. D. Ghohs and P. K. Das, Physics of Fluids, 31, 083609 (2019) https://doi.org/10.1063/1.5111577

10. S.R. Ragsdale, K.M. Grant and H.S. White, J. Am. Chem. Soc. 120, 13461 (1998).

11. K.M. Grant, J.W. Hemmert, and H.S. White, Electrochem. Commun. 1, 319 (1999).

12. A. Sugiyama, M. Hashiride, R. Morimoto, Y. Nagai, and R. Aogaki, Electrochim. Acta 49, 5115 (2004).

13. O.Y. Gorobets, V.Y. Gorobets, D.O. Derecha, and O.M. Brukva, J. Phys. Chem. C 112, 3373 (2008).

14. X. Wang, J. Zhao, Y. Hu, L. Li, and C. Wang, Electrochim. Acta 117, 113 (2014) http://dx.doi.org/10.1016/j.electacta.2013.11.100

15. X. Yang, K. Tschulik, M. Uhlemann, S. Odenbach, and K. Eckert, IEEE Trans. Mag. 50, 1 (2014).

16. S. Odenbach, Physics of Fluids, 6, 2535 (1994) https://doi.org/10.1063/1.868141

17. C.W. Tobias, M. Eisenberg, and C.R. Wilke, J. Electrochem. Soc. 99, 359C (1952).

18. R.N. O'Brian and K.S.V. Santhanam, J. Appl. Electrochem. 20, 427 (1990).

19. M. Waskaas, Acta Chem. Scand. 50, 521 (1996).

20. M. Waskaas, Acta Chem. Scand. 50, 526 (1996).

21. J.P. Chopart, O. Aaboubi, E. Merienne, A. Olivier, and J. Amblard, Energy conversion and Management 43, 365 (2002). DOI: 0.1016/S0196-8904(01)00110-8

22. Y. Yang, K.M. Grant, H.S. White, and S. Chen, Langmuir 19, 9446 (2003).

23. P.U. Arumugam, A.J. Belle, and I. Fritsch, IEEE Trans. Mag. 40, 3063 (2004).

24. A. Krause, M. Uhlemann, A. Gebert, and L. Schultz, Electrochim. Acta 49, 4127 (2004).

25. K.L. Rabah, J.P. Chopart, H. Schloerb, S. Saulnier, O. Aaboubi, M. Uhlemann, D. Elmi, and J. Amblard, J. Electroanal. Chem. 571, 85 (2004). doi:10.1016/j.jelechem.2004.04.014

26. M. Uhlemann, H. Schlörb, K. Msellak, and J.P. Chopart, J. Electrochem. Soc. 151, C598 (2004).

27. M. Uhlemann, A. Krause, J.P. Chopart, and A. Gebert, J. Electrochem. Soc. 152, C817 (2005). DOI: 10.1149/1.2073167

28. A. Bund and H.H. Kuehnlein, J. Phys. Chem. B 109, 19845 (2005).

29. A. Krause, J. Koza, A. Ispas, M. Uhlemann, A. Gebert, and A. Bund, Electrochim. Acta 52, 6338 (2007). doi:10.1016/j.electacta.2007.04.054

30. O. Lioubashevski, E. Katz, and I. Willner, J. Phys. Chem. C 111, 6024 (2007).

31. T. Weier, K. Eckert, S. Mühlenhoff, C. Cierpka, A. Bund, and M. Uhlemann, Electrochemistry Commun. 9, 2479 (2007). doi:10.1016/j.elecom.2007.07.026

32. O. Aaboubi and J. Douglade, J. Electroanal. Chem. 693, 42 (2013). http://dx.doi.org/10.1016/j.jelechem.2013.01.006

33. Y. Yu, Z. Song, H. Ge, G. Wei, and L. Jiang, Int. J. Electrochem. Sci. 10, 4812 (2015).

34. J. Newman and K.E. Thomas-Alyea, *Electrochemical systems* (John Wiley& sons, Hoboken, N.J., 2004).

35. S.R. Ragsdale and H.S. White, Anal. Chem. 71, 1923 (1999).

36. J.M.D. Coey, F.M.F. Rhen, P. Dunne, and S. McMurry, J. Solid State Electrochem. 11, 711 (2007). DOI 10.1007/s10008-006-0254-4

37. M. Waskaas, Acta Chem. Scand. 50, 516 (1996).

38. M. Waskaas and Yu.I. Kharkats, J.Phys.Chem. 103, 4876 (1999).

39. N.S. Perov, P.M. Sheverdyaeva, and M. Inoe, J. Appl. Phys. 91, 8557 (2002).

40. A. Rucinskiene, G. Bikulcius, L. Gudaviciute, and E. Juzeliunas, Electrochem. Commun. 4, 86 (2002).

41. A. Dass, J.A. Counsil, X. Gao, and N. Leventis, J. Phys. Chem. B 109, 11065 (2005).

42. F.M.F. Rhen and J.M.D. Coey, J. Phys. Chem. C111, 3412 (2007).

43. Z. Lu and W. Yang, Corrosion Science 50, 510 (2008).

44. N. Leventis and X. Gao, J. Am. Chem. Soc. 125, 1079 (2002).

45. N. Leventis and A. Dass, J. Am. Chem. Soc. 127, 4988 (2005).

46. N. Leventis, A. Dass, and N. Chandrasekaran, J Solid State Electrochem. 11, 727 (2007). DOI 10.1007/s10008-006-0193-0

47. M. Waskaas, J. Phys. Chem. 97, 6470 (1993).

48. K. Mogi, T. Sakihama, N. Hirota, and K. Kitazava, J. Appl. Phys. 85, 5714 (1999).

49. J.R. Reitz, F.J. Milford, and R.W. Christy, *Foundations of lectromagnetic theory* (Addison-Wesley. Reading, MA., 1993).

50. S.S. Bhatnagar and K.N. Mathur, *Physical principles and applications of magnetochemistry* (MacMillan, London, 1935).

51. L.N. Mulay, *Magnetic susceptibility* (John Wiley and sons, New York, 1963).

52. H. Scott Fogler, *Elements of Chemical Reaction Engineering* (Prentice Hall, Upper Saddle River, N.J., 2006).

53. C.J. Geankoplis, *Tranport Processes and Unit Operations* (Prentice-Hall, Englewood Cliffs, NJ., 1983).

54. F.W. Sears, *An Introduction to Thermodynamics, the kinetic Theory of Gases and Statistical mechanics* (Addison-Wesley, Reading, MA., 1971).

55. R.L. Boylestad, *Introductory circuit analysis* (Pearson, Boston, MA, 2016).

56. V.E. Mablekos, *Electric machine theory for power engineers* (Harper & Row, New York, 1980).

57. B. Hegde and N.S. Dinesh, Microsyst. Technol. 23, 5023 (2017). DOI 10.1007/s00542-017-3363-3

58. Yu Kharkats, Russian J. Electrochemistry 35, 825 (1999).

59. IMSL International Mathematical and Statistics Library, Volume 2, 1991.

60. https://en.wikipedia.org/wiki/Hagen%E2%80%93Poiseuille equation#Equation June 24 2019.

61. https://mathworld.wolfram.com/BesselFunctionZeros.html June 24

2019.

62. H.R. Nettleton and F.R.S. Sugden, *The Magnetic Susceptibility of Nickel chloride* (Birbeck College and University College, London, 1939).

Symbol List

A_{lm} : cross-sectional area of the membrane covered by liquid, m^2
B : constant magnetic field in the x-direction, T
c : concentration of Ni ions in distilled water, mol/dm^3 (M)
D : diffusion coefficient for Ni ions in distilled water, m^2/s
E : energy density stored in the magnetic field, J/m^3
F : magnetic force per unit liquid volume, N/m^3
g : acceleration of gravity, m/s^2
H_{lm} : height of the membrane covered with liquid, m
j : mole flux of the Ni ions, mol/m^2s
J_n : Bessel functions
K : constant = total number of moles of Ni ions in the system, mol
k : mass transfer coefficient, m/s
k_m : parameter with magnetic properties, J/mol
k_v : parameter with magnetic, fluid and geometrical properties,$m^4/mol/s$
L_m : length of the membrane, m
n : number of moles of Ni ions at time t, mol
p : static pressure, Pa
Q : heat per unit liquid volume, J/m^3
R : pore radius in the membrane, m
r : radial distance in a cylindrical pore, m
$\overline{\mathcal{R}}$: average magnetic reluctance in the membrane, 1/H
Re : Reynolds number
t : time, s
td : delay time specified by the user or determined by regression, s
U : internal energy per unit liquid volume, J/m^3
v_m : velocity of the Ni ions in the membrane generated by F_m, m/s
V : liquid volume, m^3
W : work done on the system per unit liquid volume, J/m^3
W_m : width of the membrane, m
x : direction of the diffusion flux and the magnetic field, m
y : opposite direction of x, m
z : local liquid height, m

Greek Letters

γ : cubic polynomial (mol/m^3)
ε_m : porosity (void) of the membrane
η : kinematic viscosity of the liquid, m^2/s

κ : magnetic volume susceptibility
λ_n : eigenvalue
μ_0 : magnetic permeability for vacuum, $4\pi \cdot 10^{-7}$H/m = $12.57 \cdot 10^{-7}$ H/m
ρ : liquid density, kg/m^3
χ_{mol} : magnetic molar susceptibility of Ni ions, m^3/mol

Subscripts
c : channel, part of chamber 1
D : diffusion
eff : effective
k : kinetic
l : liquid
m : magnetic or membrane
mol : mole of Ni ions
ov : overall
p : potential
r : reservoir (chamber 1 including the channel in front of membrane)
s : solution
v : convection
0 : initial or vacuum
1 : chamber 1 (reservoir + channel)
2 : chamber 2

Appendix A. Calculation of freeboard, liquid heights and volumes

Initially, 29.0 ml of 1M solution was added to chamber 1, and 0.6 ml distilled water was added to chamber 2. Since the liquid volumes communicate, the height of the freeboard,F, was constant and equal in both the membrane and in the two chambers. When F has been calculated, the liquid volume in chamber 1, 2 and the membrane can be calculated. The empty volumes of the reservoir, the channel, chamber 1, the membrane and chamber 2 are given by

$$V_r = L_r W_r H_r \ , V_c = L_c W_c H_c \ , \ V_1 = V_r \ + V_c \ , V_m = \ \varepsilon_m L_m W_m H_m , V_2 = L_2 W_2 H_2 \qquad \text{(A1)}$$

Based on the geometry data in Table 3 in Appendix B, the total volume balance of the liquid solution becomes

$$(H_r - F)L_r W_r \ + \ (H_c - F)L_c W_c \ + \ (H_m - F)\varepsilon_m L_m W_m \ + (H_2 - F)L_2 W_2 \ = \ 29.0 \ + 0.6 \qquad \text{(A2)}$$

Equation (A2) is solved with respect to the depth of the freeboard F. The result is

$$F = \frac{V_r + V_c + V_m + V_2 - 29.0 - 0.6}{L_r W_r + L_c W_c + \varepsilon_m L_w W_m \ + L_2 W_2} \qquad \text{(A3)}$$

When the depth of the freeboard F is known, the liquid height in each chamber and in the membrane is calculated from

$$H_{lr} = H_r - F, H_{lc} = H_c - F, H_{l1} = H_1 - F, \; H_{l2} = H_2 - F, H_{lm} = H_m - F \quad \text{(A4)}$$

The corresponding liquid volumes are

$$V_{lr} = L_r W_r H_{lr}, \; V_{lc} = L_c W_c H_{lc}, \; V_{l1} = V_{lr} + V_{lc}, \; V_{lm} = \varepsilon_m L_m W_m H_{lm}, \; V_{l2} = L_2 W_2 H_{l2} \quad \text{(A5)}$$

Appendix B. Equipment data

The electromagnet can produce a constant magnetic field between 0 and 0.8 T. The dimension of the system is shown in Table 3.

Table 3. Equipment data.

Description	Name	Dimension (cm)
Reservoir in chamber 1	Reservoir	
Material	Teflon	
Freeboard	F	1.1
Length	L_r	1.1
Width	W_r	9.0
Height	H_r	4.0
$L_r W_r H_r$	V_rv	39.6 (cm^3)
Liquid height	$H_{lr} = H_r - F$	2.9
$L_r W_r H_{lr}$	V_{lr}	28.7 (cm^3)
Channel in chamber 1	Channel	
Material	Teflon	
Freeboard	F	1.1
Length	L_c	0.5
Width	W_c	0.4
Height	H_c	3.0
$L_c W_c H_c$	V_c	0.6 (cm^3)
Liquid height	$H_{lc} = H_c - F$	1.9
$L_c W_c H_{lc}$	V_{lc}	0.38 (cm^3)
Chamber 2		
Material	Teflon	
Freeboard	F	1.1
Length	L_2	0.6
Width	W_2	0.4
Height	H_2	3.0
$L_2 W_2 H_2$	V_2	0.72 (cm^3)
Liquid height	$H_{l2} = H_2 - F$	1.9
$L_2 W_2 H_{l2}$	V_{l2}	0.46 (cm^3)

Membrane	GSTF 02500	
Material	Cellulose esters	
Freeboard	F	1.1
Length	L_m	150 (μm)
Width	W_m	0.4
Height	H_m	3.0
Void	ε_m	0.75 (-)
$\varepsilon_m L_m W_m H_m$	V_m	$1.35 \cdot 10^{-4}$ (cm^3)
Liquid height	$H_{lm} = H_m - F$	1.9
$\varepsilon_m L_m W_m H_{lm}$	V_{lm}	$8.55 \cdot 10^{-5}$ (cm^3)
$\varepsilon_m W_m H_{lm}$	A_{lm}	0.57 (cm^2)
Pore diameter	D_p	0.22 (μm)
Electromagnet	Open frame Newport	
Gauss meter	RFL Model 750	
Accuracy	1 mT	
Magnetic field	B	0 – 820 mT
Circular poles	D_{em}	10 (cm)
Gap between the pole shoes	G_p	3 (cm)
Photometer	Photodyne, Model 44XLA	
Laser	Spectra Physics Model 133 Laser, He-Neon	

Appendix C. The velocity in the membrane generated by magnetic field B

The hydraulic static pressure, p, is constant in all cases simulated in this article, and consequently, $\nabla p = 0$. If, in addition the magnetic field $B = 0$, then $F_m = 0$, and the mass average velocity is $\boldsymbol{v} = 0$. In that case only diffusion and counter diffusion occur in the membrane. If $F_m \neq 0$, a local mass average velocity v is developed in the membrane. For constant electrolyte density, ρ, it follows from the equation of continuity that $\boldsymbol{v} \cdot \nabla \boldsymbol{v} = 0$. The tortuosity τ of the membrane is unknown. Hence, the diffusion coefficient, D, is regarded the effective diffusion coefficient.

The mass average velocity in a pore tube of the membrane, v, is written in cylinder coordinates. For constant density ρ and kinematic viscosity, η, the dynamic momentum balance can be written

$$\frac{\partial \boldsymbol{v}}{\partial t} = \frac{F_m}{\rho} + \eta \left(\frac{\partial^2 v}{\partial r^2} + \frac{1}{r} \frac{\partial v}{\partial r} \right) \tag{C1}$$

This is the dynamic momentum balance for the velocity of the Ni ions in the membrane. It leads to the well-known Hagen-Poiseuille formula for laminar flow in a cylinder. The initial and boundary conditions are

$$v(r,0) = 0 \tag{C2}$$

$$v(R,t) = 0 \ , \ \frac{\partial v(0,t)}{\partial r} = 0 \tag{C3}$$

In our case, $R = R_p$, the radius of a pore in the membrane. If F_m is constant, the solution of Eq. (C1), with initial condition Eq. (C2) and boundary conditions Eq. (C3), reads:[60]

$$v(r,t) = F_m \frac{(R^2-r^2)}{4\eta\rho} - F_m \frac{2R^2}{\eta\rho} \sum_{n=1}^{\infty} \frac{1}{\lambda_n^3} \frac{J_0(\frac{\lambda_n r}{R})}{J_1(\lambda_n)} \exp\left(-\lambda_n^2 \frac{\eta t}{R^2}\right) \tag{C4}$$

The eigenvalues λ_n are the solution of $J_0(\lambda_n) = 0$. The five first eigenvalues are listed as 2.4048, 5.5201, 8.6537, 11.7915 and 14.9309.[61]

When the factor $\exp\left(-\lambda_1^2 \frac{\eta t}{R^2}\right)$ approaches zero, the velocity approaches steady-state, and the last term in Eq. (C4) goes to zero. After one second the factor becomes

$$\exp\left(-\lambda_1^2 \frac{\eta t}{R^2}\right) = \exp\left(-2.4048^2 . \frac{10^{-6} \cdot 1}{(0.11 \cdot 10^{-6})^2}\right) = \exp\left(-4.7794 \cdot 10^8\right) \approx 0$$

Hence, in our case, steady-state occurs almost immediately. The remaining first term is the Hagen-Poiseuille steady-state velocity for laminar flow in a cylinder in the membrane of radius $R = R_{pore}$ and reads.

$$v(r) = F_m \frac{(R^2-r^2)}{4\rho\eta} \tag{C5}$$

The average velocity of the liquid solution is

$$v_m = F_m \frac{R^2}{8\rho\eta} \tag{C6}$$

The Reynolds number for flow in a cylinder with diameter $D = D_{pore}$ is

$$Re = \frac{v_m D}{\eta} \tag{C7}$$

The flow is laminar if Re < 2300. In our case, the typical Reynolds number is

$Re = \frac{10^{-6} \cdot 0.22 \cdot 10^{-6}}{10^{-6}} = 0.22 \cdot 10^{-6} \approx 0.$
Consequently, Eq. (C6) is valid for all cases in this study.

From Eq. (C8) it follows that

$$F_m = \frac{\mathrm{dE}_m}{\mathrm{dx}} \approx -\frac{\chi_{\mathrm{mol}} \mathrm{B}^2}{2\mu_0} \frac{\partial \mathrm{c}}{\partial \mathrm{x}} \tag{C8}$$

Combining Eq. (C6) and Eq. (C8), it follows that the derivative of the kinetic energy per unit volume, E_k, is

$$\frac{dE_k}{dx} = \frac{d}{dx}\left(\frac{1}{2}\rho v_m^2\right) = \rho \frac{dv_m}{dx} = -\frac{\rho R^2 B^2 \chi_{\mathrm{mol}}}{16\eta\mu_0} \frac{d^2\mathrm{c}}{\mathrm{dx}^2} \tag{C9}$$

Hence, it follows that

$$\frac{dE_k/dx}{dE_m/dx} = \frac{\rho R^2}{8} \frac{d^2\mathrm{c}/\mathrm{dx}^2}{dc/dx} = 1.82 \cdot 10^{-12} \frac{d^2\mathrm{c}/\mathrm{dx}^2}{dc/dx} \ll 1 \tag{C10}$$

This means that the total energy E per unit liquid volume is

$$E = E_m + U + E_k + E_p \tag{C11}$$

$$E_k = \frac{1}{2}\rho v_m^2 \tag{C12}$$

$$E_p = \rho g z \tag{C13}$$

In Eq. (C11) , *U* is the internal energy per unit liquid volume, E_k is the kinetic energy per unit liquid volume, and E_p is the potential energy per unit liquid volume. The temperature is constant so the change in internal energy per unit volume, dU/dx = 0. Since liquid level z is constant, the change in the potential energy per unit liquid volume, $dE_p/dx = 0$.

The infinitesimal change in E with respect to x is in our case

$$\frac{\mathrm{dE}}{dx} = \frac{dE_m}{dx} + \frac{dU}{dx} + \frac{dE_k}{dx} + \frac{dE_p}{dx} \tag{C14}$$
$$\frac{\mathrm{dE}}{dx} = \frac{dE_m}{dx} + 0 + \frac{dE_k}{dx} + 0 = \frac{dE_m}{dx} + \frac{dE_k}{dx} \tag{C15}$$

When Eq. (C10) is used, Eq. (C15) becomes

$$\frac{\mathrm{dE}}{dx} \approx \frac{dE_m}{dx} \text{ and } \mathrm{dE} \approx dE_m \tag{C16}$$

Hence, the total energy per unit liquid volume, E, is in our case approximately equal to the magnet energy per unit liquid volume, E_m.

Appendix D. The magnetic susceptibility of the aqueous Ni solution

Ni is paramagnetic, and water is diamagnetic.[62] The Ni-ions are accompanied by Cl-ions due to the Coulomb force. Both type of ions move in the direction of the magnetic field while diamagnetic water molecules move in the opposite direction with negligible velocity. The mass magnetic susceptibility for 100% Ni in cgs units is given by.

$$\chi_{mass}^{cgs} = \frac{0.01003}{T} = 3.4215 \cdot 10^{-5} \quad \text{at 20 °C} \qquad (\text{cm}^3/\text{g}) \tag{D1}$$

The liquid temperature T is given in Kelvin. The corresponding magnetic molar susceptibility for 100 % Ni in cgs units becomes

$$\chi_{mol}^{cgs} = \chi_{mass}^{cgs} M_i = 3.4215 \cdot 10^{-5} \cdot 129.60 = 4.434 \cdot 10^{-3} \quad (\text{cm}^3/\text{mol}) \tag{D2}$$

To convert the magnetic molar susceptibility of 100 % Ni from cgs to SI units the following relationship must be used

$$\chi_{mol} = 4\pi \cdot 10^{-6} \chi_{mol}^{cgs} = 4\pi \cdot 10^{-6} \cdot 4.434 \cdot 10^{-3} = 5.5719 \cdot 10^{-8} \qquad (\text{m}^3/\text{mol}) \tag{D3}$$

The magnetic mass susceptibility for 100 % water at 20 °C in cgs units is:[50]

$$\chi_{mass,w}^{cgs} = -0.720 \cdot 10^{-6} \quad (\text{cm}^3/\text{g}) \tag{D4}$$

The corresponding magnetic molar susceptibility for 100 % water in cgs units is then

$$\chi_{mol,w}^{cgs} = \chi_{mass,w}^{cgs} M_w = -0.720 \cdot 10^{-6} \cdot 18.02 = -1.297 \cdot 10^{-5} \quad (\text{cm}^3/\text{mol}) \tag{D5}$$

To convert the magnetic molar susceptibility of distilled water from cgs to SI units the following relationship is used

$$\chi_{mol,w} = 4\pi \cdot 10^{-6} \chi_{mol,w}^{cgs} = 4\pi \cdot 10^{-6} \cdot (-1.297 \cdot 10^{-5}) = -1.6299 \cdot 10^{-10} \quad (\text{m}^3/\text{mol}) \tag{D6}$$

The ratio between the magnetic molar susceptibility of pure Ni and distilled water becomes

$$\frac{\chi_{mol}}{\chi_{mol,w}} = \frac{5.5719 \cdot 10^{-8}}{-1.6299 \cdot 10^{-10}} = -341.86 \tag{D7}$$

This ratio shows that the absolute value of the magnetic molar susceptibility of Ni is much larger than the magnetic molar susceptibility of distilled water. Hence, the influence of the magnetic field B on distilled water can be neglected, and water is assumed to be approximately stagnant in this article.

Appendix E. Derivation of the simplified partial differential equation.

The concentration $c_2(t)$ of $NiCl_2$ in chamber 2 is a function of the flux j out of the membrane at x = L_m. Initially, and at steady state $\frac{dc}{dx}$=0 at x = L_m. When t increases both $c_2(t)$ and $c(Lm,t)$ increases due to the boundary condition $c(Lm,t)=c_2(t)$. The value of $c_2(t)$ is much larger than the absolute value of $\frac{dc}{dx}$ at x = L_m when time increases. To discuss this further, a Taylor expansion for $\frac{dc}{dx}$ to first order around x = a is obtained.

The Taylor expansion reads

$\frac{dc(x,t)}{dx} \approx \frac{dc(a,t)}{dx} + \frac{d^2c(a,t)}{dx^2}(\mathrm{x}-\mathrm{a}) = \mathrm{b(t)} + \frac{d^2c(a,t)}{dx^2}\Delta x$. When the expansion is inserted

into the expression above with $\frac{dc(x,t)}{dx} \approx \frac{\Delta c}{\Delta x}$, the result is

$$k_v\left[c\frac{d^2c}{dx^2}+\left(\frac{dc}{dx}\right)^2\right] \approx k_v\left[c\frac{\left(\frac{\Delta c}{\Delta x}-b\right)}{\Delta x}+\left(\frac{\Delta c}{\Delta x}\right)^2\right] = k_v\left[\frac{\Delta c}{\Delta x}\left(\frac{c}{\Delta x}-\frac{cb}{\Delta x\frac{\Delta c}{\Delta x}}+\frac{\Delta c}{\Delta x}\right)\right]$$

The concentration c(x,t) in the membrane decreases with x. Hence $\frac{\Delta c}{\Delta x} < 0$ and b <= 0, where b = 0 initially and at steady state. The ratio $r = \frac{b}{\frac{\Delta c}{\Delta x}} < 1$. It is inserted into the expression above. The result becomes

$$k_v\left[c\frac{d^2c}{dx^2}+\left(\frac{dc}{dx}\right)^2\right] \approx k_v\left[\frac{\Delta c}{\Delta x}\left(\frac{c}{\Delta x}-\frac{cr}{\Delta x}+\frac{\Delta c}{\Delta x}\right)\right] = k_v\left[\frac{\Delta c}{\Delta x}\left(\frac{c(1-r)}{\Delta x}+\frac{\Delta c}{\Delta x}\right)\right]$$

As c(a,t) increases with time when x > 0, it follows that $c(1-r) \gg \Delta c$. In points x within the membrane which may have large changes in the local gradient $\frac{dc}{dx}$ at time t, it follows that $r \approx 0$. When $\Delta x \to 0$, the result becomes

$k_v\left[c\frac{d^2c}{dx^2}+\left(\frac{dc}{dx}\right)^2\right] \approx k_v\left[c\frac{\Delta c}{\Delta x}\frac{(1-r)}{\Delta x}\right] \approx k_v c\frac{d^2c}{dx^2}$, in points x = a, where $r \approx 0$, $\frac{dc}{dx} \gg b$

$k_v\left[c\frac{d^2c}{dx^2}+\left(\frac{dc}{dx}\right)^2\right] = 0$, in points where $r = 1$, typically at x = L_m at steady-state.

Initially and at steady state $\frac{dc}{dx} = 0$ and $\frac{d^2c}{dx^2}$ = 0.

Hence, the quadratic term $\left(\frac{\Delta c}{\Delta x}\right)^2$ can be ignored. This explains why the simplified Eq. (25b) in the article is a good approximation to Eq. (24) and Eq. (25a) given the boundary condition at x = L_m.

Appendix F. The measurements in Waskaas 1993.[47]

Table 4. Experimental values for Fig. 4.

Concentration 1 mol dm^{-3} and 0 T

t (s)	c mol dm^{-3}	Δc mol dm^{-3}
0	0.000	0.000
150	0.016	0.005
338	0.097	0.008
525	0.191	0.012
705	0.263	0.015

Concentration 1 mol dm^{-3} and 0.67 T

t (s)	c mol dm^{-3}	Δc mol dm^{-3}
0	0.000	0.000
150	0.035	0.012
279	0.117	0.021
525	0.262	0.033
705	0.356	0.037

Concentration 1 mol dm^{-3} and 0.82 T

t (s)	c mol dm^{-3}	Δc mol dm^{-3}
0	0.000	0.000
150	0.083	0.022
223	0.157	0.026
400	0.283	0.033
705	0.477	0.037

Table 5. Experimental values for Fig. 5.

Concentration 0.5 mol dm^{-3} and 0 T

t (s)	c mol dm^{-3}	Δc mol dm^{-3}
0	0.000	0.000
150	0.017	0.004
279	0.064	0.005
525	0.150	0.008
705	0.204	0.010

Concentration 0.5 mol dm^{-3} and 0.67 T

t (s)	c mol dm^{-3}	Δc mol dm^{-3}
0	0.000	0.000
150	0.017	0.001
463	0.160	0.007
525	0.196	0.010
705	0.287	0.019

Concentration 2 mol dm^{-3} and 0 T

t (s)	c mol dm^{-3}	Δc mol dm^{-3}
0	0.000	0.000
150	0.030	0.005
412	0.263	0.017
525	0.390	0.029
705	0.580	0.044

Concentration 2 mol dm^{-3} and 0.67 T

t (s)	c mol dm^{-3}	Δc mol dm^{-3}
0	0.000	0.000
150	0.053	0.013
337	0.287	0.022
525	0.545	0.026
705	0.763	0.027

Figure captions

Fig. 1 Experimental details: a. Experimental setup, b. Side view of the exposure chamber used in the experimental setup, c. Top view of the exposure chamber used in the experimental setup.

Fig. 2. I. Principle sketch of the experimental setup. A paramagnetic electrolyte diffuses from chamber 1, concentration c_1, through an inert membrane into chamber 2, concentration c_2 at a time t after start of diffusion. A horizontal uniform magnetic field B is applied perpendicular to the membrane. II. An equivalent concentration profile through the system.

Fig. 3. a. Case A: constant magnetic field B points in the positive x-direction. b. Case B: constant magnetic field B points in the negative x-direction.

Fig. 4. Comparison of measured and simulated values in the 1 M case.

Fig. 5. Comparison of measured and simulated values for 0.5 M and 2 M with B = 0.67 T.

Fig. 6. Comparison of the numeric solution and the simplified numeric solution. Simulation time is 12000 s, which is well beyond the time needed to reach steady-state, as shown in the figure. Isothermal conditions are assumed for the whole time span. The black and blue line is almost identical and difficult to distinguish without zooming, and so is the red and green line.

a)

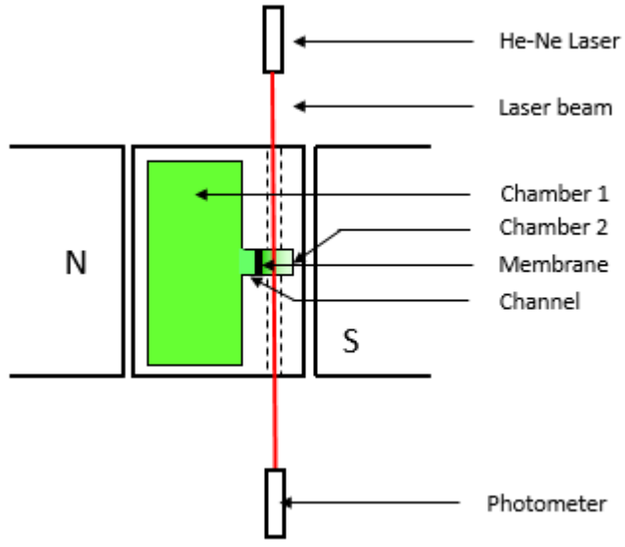

b)

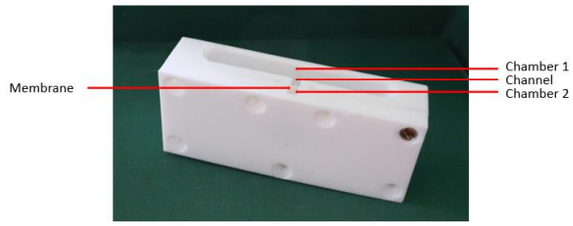

c)

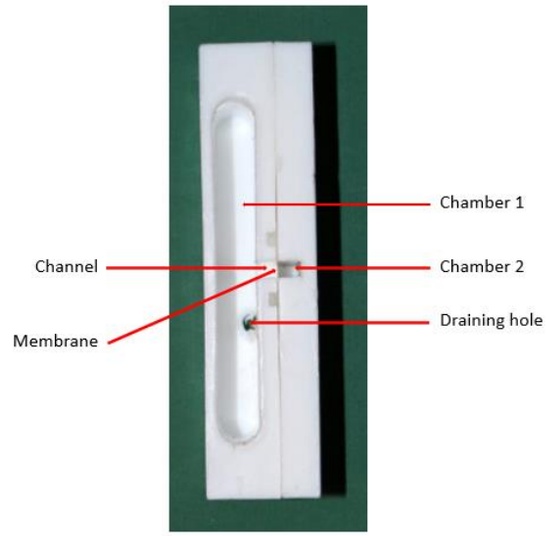

Fig. 1.

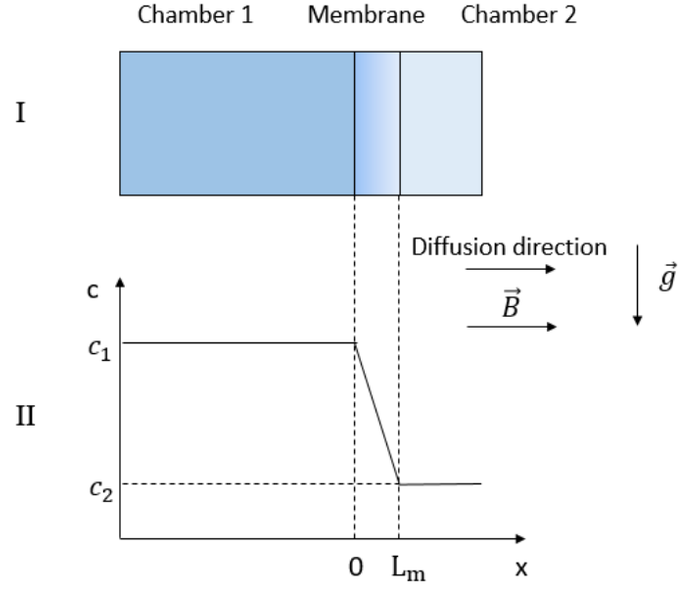

Fig. 2.

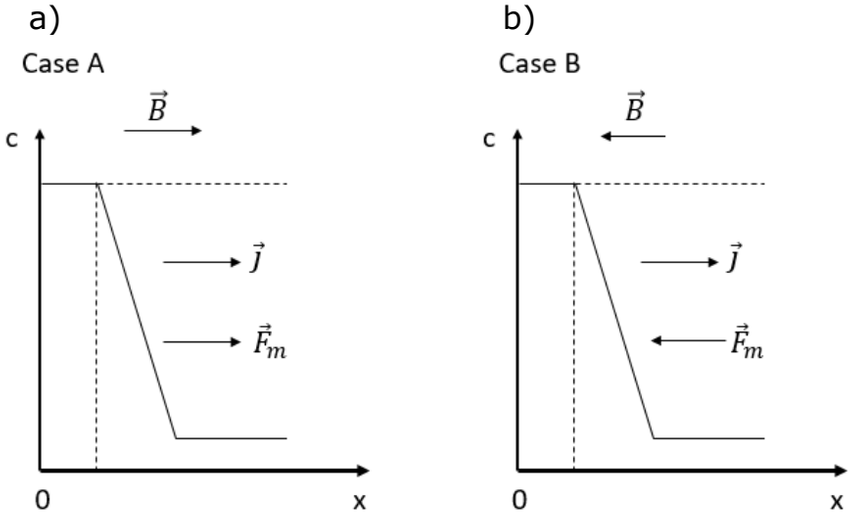

Fig. 3.

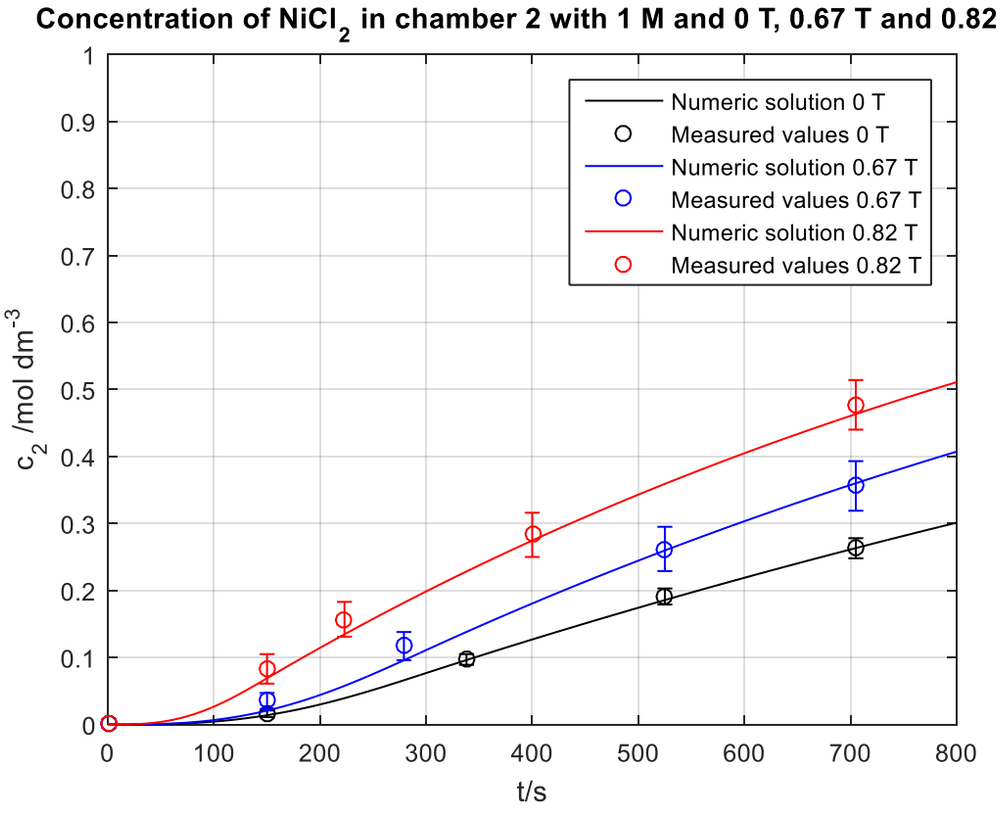

Fig. 4.

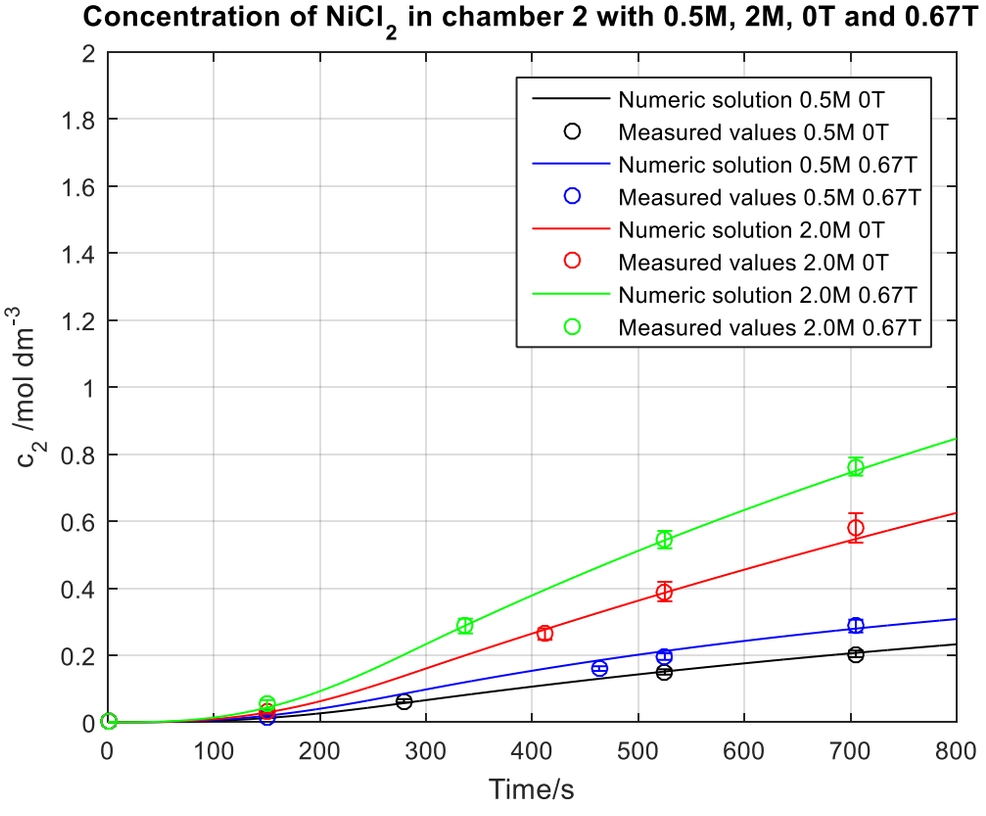

Fig. 5.

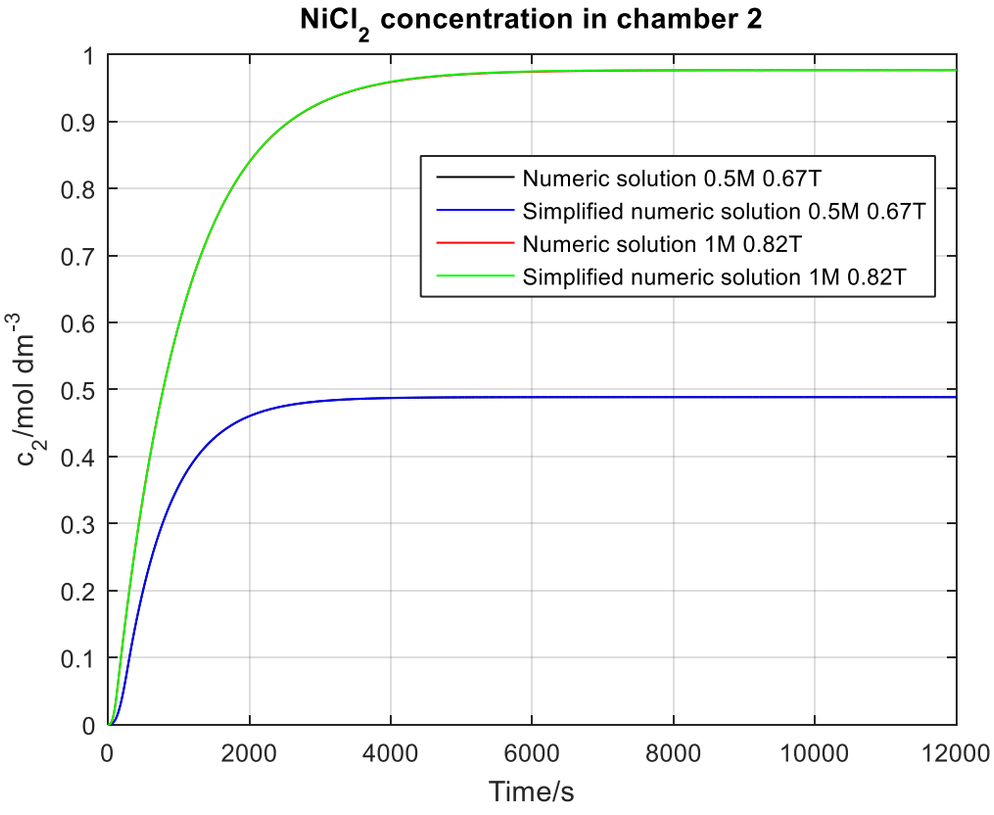

Fig.6.

a)

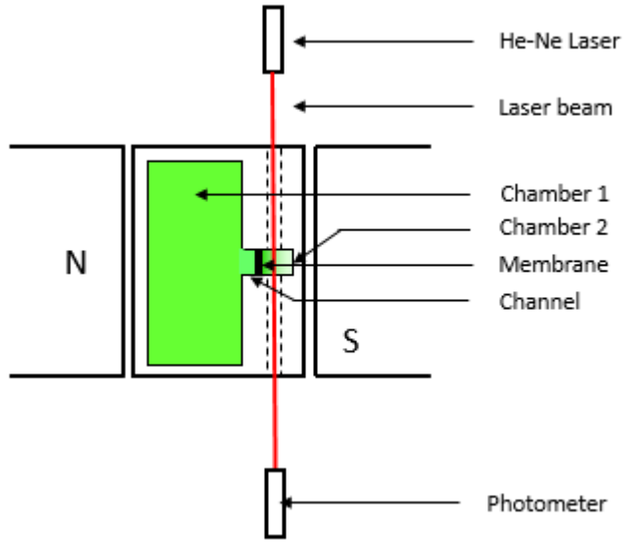

b)

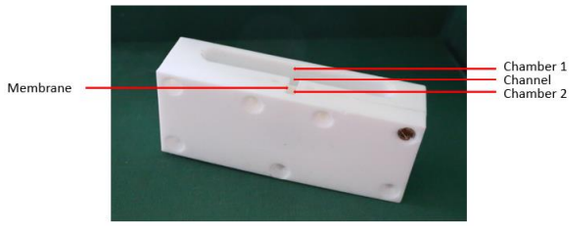

c)

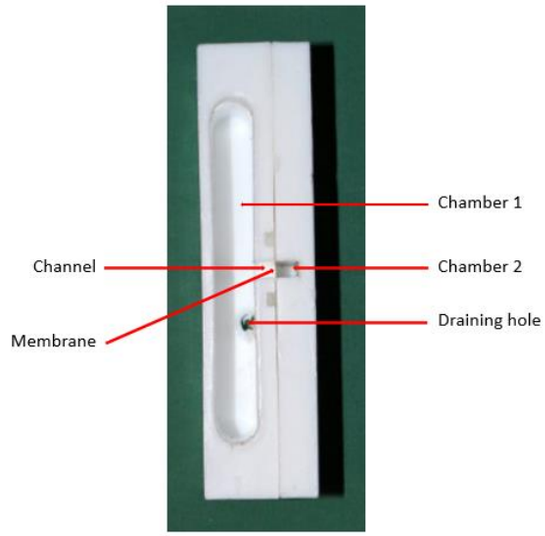

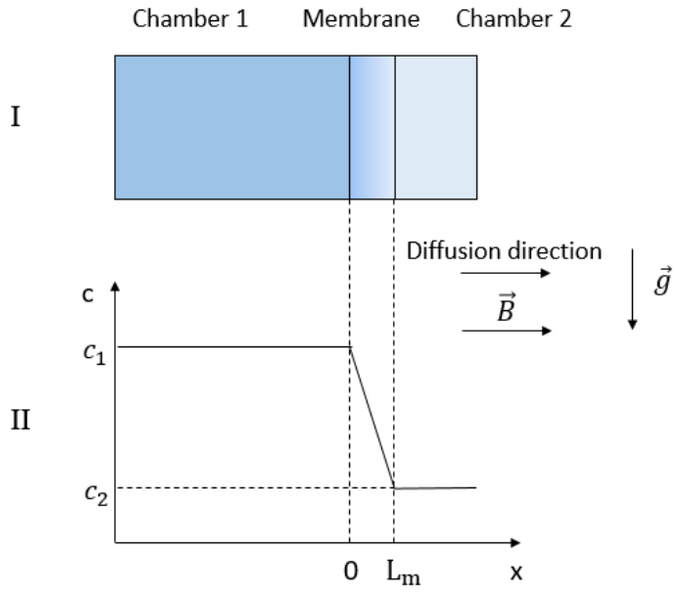

Physics of Fluids

AIP Publishing

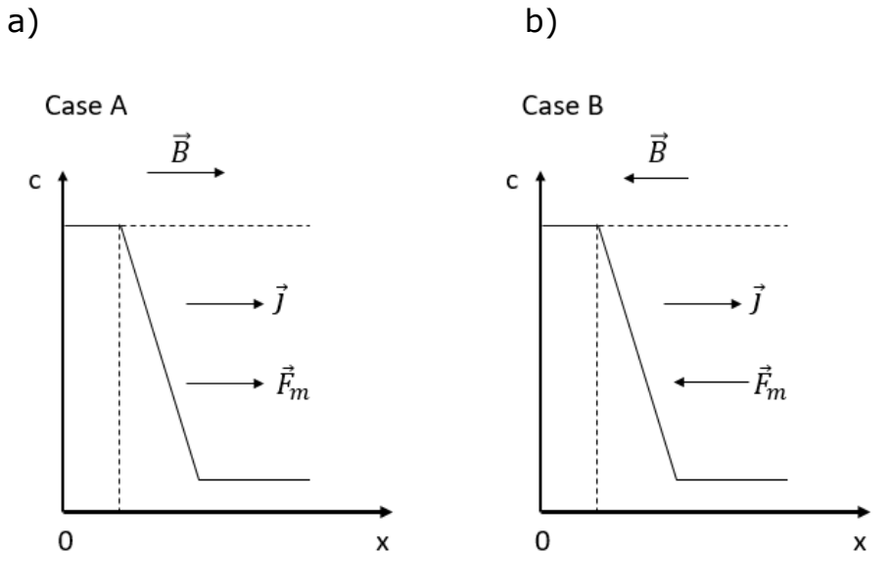

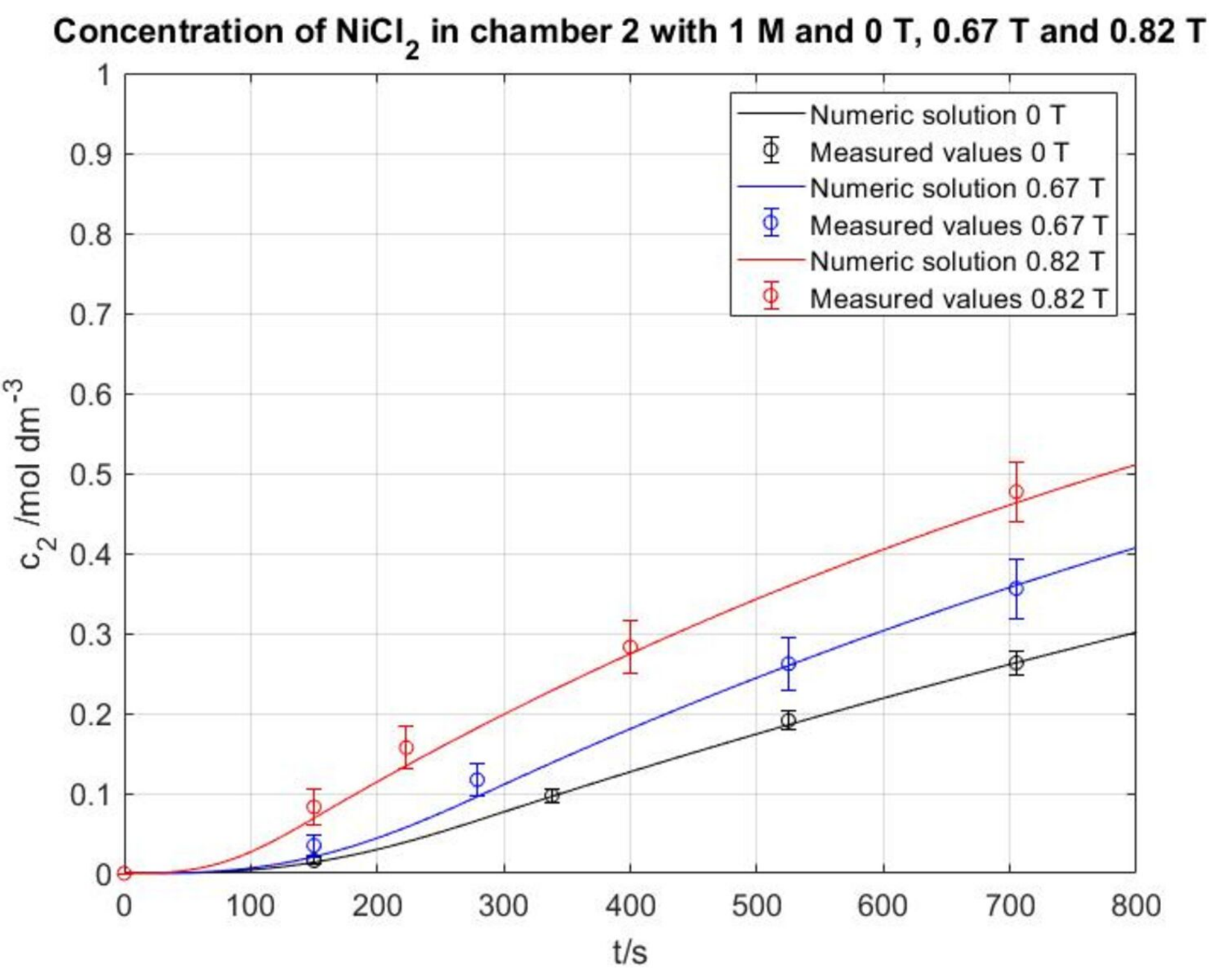
Concentration of NiCl2 in chamber 2 with 1 M and 0 T, 0.67 T and 0.82 T
Numeric solution 0 T
Measured values 0 T
Numeric solution 0.67 T
Measured values 0.67 T
Numeric solution 0.82 T
Measured values 0.82 T
c2 /mol dm-3
t/s
0
0.1
0.2
0.3
0.4
0.5
0.6
0.7
0.8
0.9
1
0
100
200
300
400
500
600
700
800

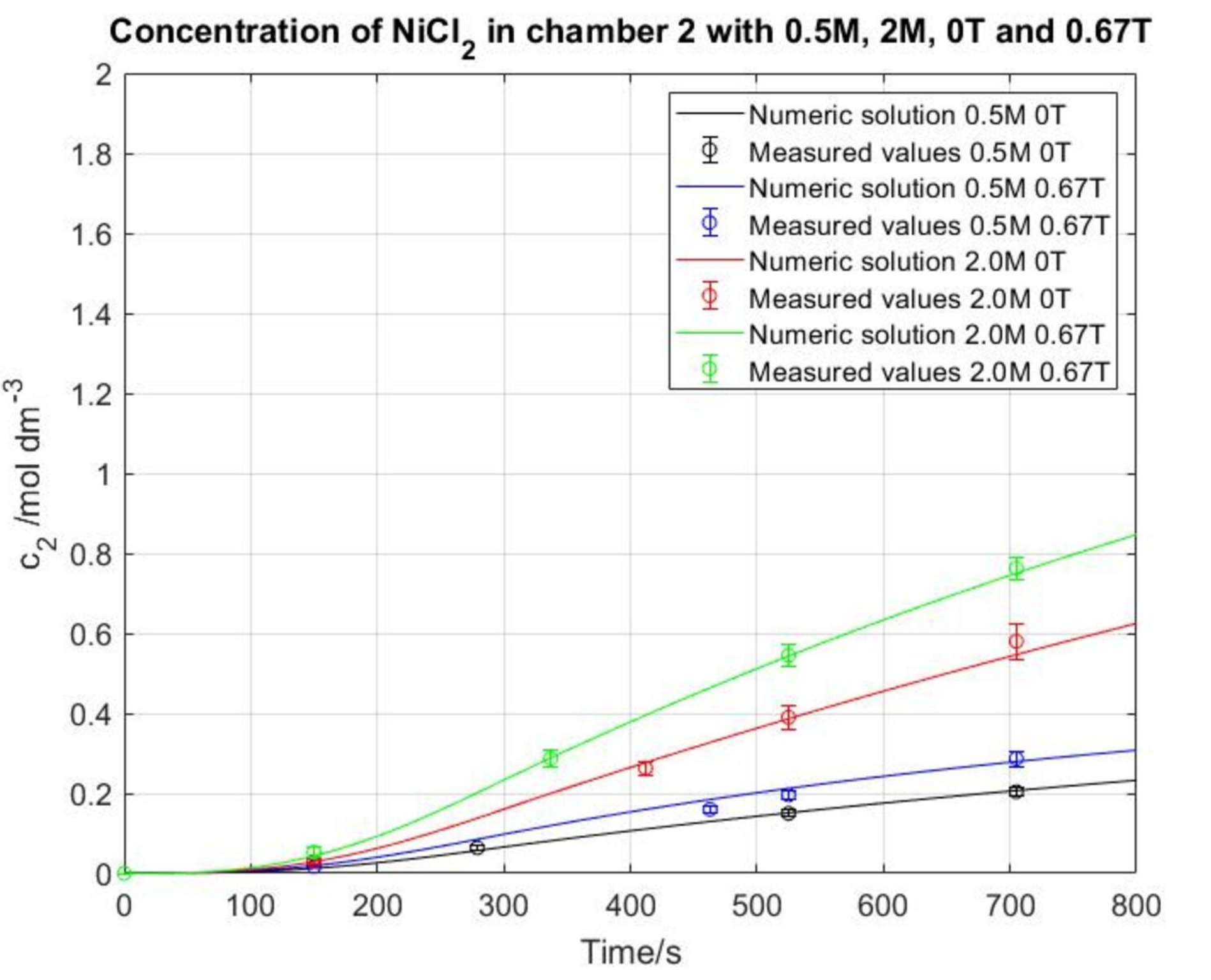
Concentration of NiCl2 in chamber 2 with 0.5M, 2M, 0T and 0.67T
Numeric solution 0.5M 0T
Measured values 0.5M 0T
Numeric solution 0.5M 0.67T
Measured values 0.5M 0.67T
Numeric solution 2.0M 0T
Measured values 2.0M 0T
Numeric solution 2.0M 0.67T
Measured values 2.0M 0.67T
c2 /mol dm-3
Time/s
0
0.2
0.4
0.6
0.8
1
1.2
1.4
1.6
1.8
2
0
100
200
300
400
500
600
700
800

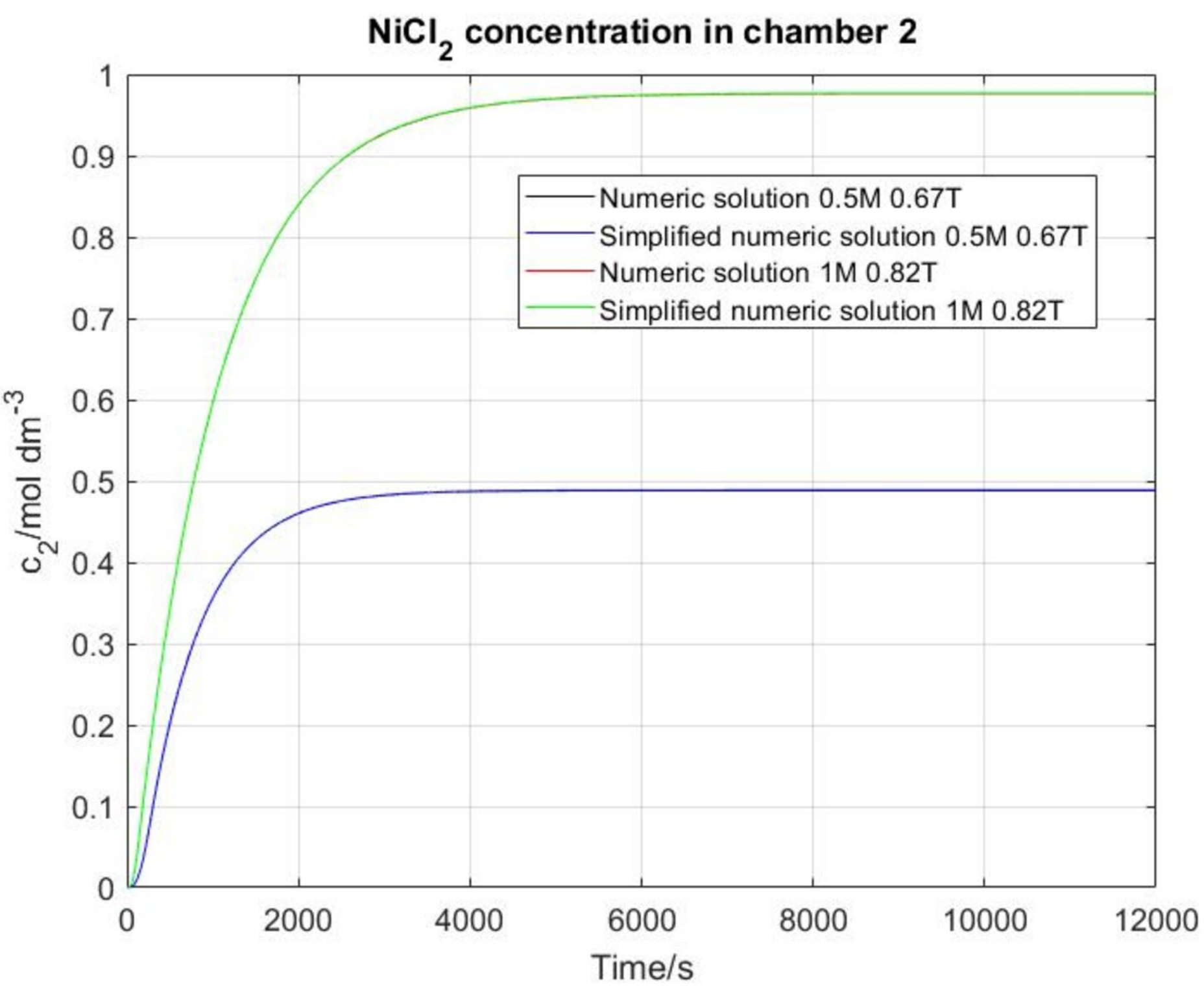
NiCl2 concentration in chamber 2
Numeric solution 0.5M 0.67T
Simplified numeric solution 0.5M 0.67T
Numeric solution 1M 0.82T
Simplified numeric solution 1M 0.82T
c2/mol dm-3
Time/s
0
0.1
0.2
0.3
0.4
0.5
0.6
0.7
0.8
0.9
1
0
2000
4000
6000
8000
10000
12000